

Anisotropic heat transport in magnetized plasmas

D. del-Castillo-Negrete¹, D. Blazevski², and L. Chacón¹

¹ Oak Ridge National Laboratory, Oak Ridge, TN 37831-6169, USA

² University of Texas at Austin, TX 78702, USA

I. Introduction. Heat transport in magnetized plasmas

is a problem of fundamental interest in controlled fusion. Three issues make this problem particularly difficult: (i) The extreme anisotropy between the parallel (i.e., along the magnetic field), χ_{\parallel} , and the perpendicular, χ_{\perp} , conductivities; (ii) magnetic field lines chaos; and (iii) nonlocal parallel flux closures in the limit of small collisionality. Motivated by the extreme anisotropy encountered in fusion plasmas, in which the ratio $\chi_{\parallel}/\chi_{\perp}$ may exceed 10^{10} , we focus on the study of purely parallel transport, i.e., $\chi_{\perp} = 0$. In Refs.[1,2] we proposed a Lagrangian-Green's function (LG) method (see Fig.1) and applied it to study transport in magnetic field configurations with monotonic q profiles. The LG method bypasses the need to discretize the transport operators on a grid and allows the integration of the parallel transport equation without perpendicular pollution, while preserving the positivity of the temperature field. The method is applicable to local and non-local parallel flux closures in integrable, weakly chaotic, and fully chaotic magnetic fields. The goal of this paper is to apply the LG method to study parallel transport in reversed shear magnetic field line configurations [3].

II. The Lagrangian-Green's function method. Our starting point is the heat transport equation for a constant density plasma, $\partial_t T = -\nabla \cdot (\mathbf{q}_{\perp} + q_{\parallel} \hat{\mathbf{b}}) + S$, where $\hat{\mathbf{b}} = \mathbf{B}/|B|$ is the unit magnetic vector field, and S is a source. As mentioned before, we limit attention to parallel transport, i.e. $\mathbf{q}_{\perp} = 0$, and assume a closure relation between the parallel flux, q_{\parallel} , and the temperature, T , of the form, $q_{\parallel} = \chi_{\parallel} \mathcal{Q}[T, \nabla T]$. Depending on the physics of the closure model, \mathcal{Q} can be a linear or a non-linear, differential or integro-differential operator. In the case of local (diffusive) parallel closures, $\mathcal{Q}[T, \nabla T] = -\partial_s T$, where $\partial_s = \hat{\mathbf{b}} \cdot \nabla$, is the directional derivative along the field line. In the case of non-local parallel closures we assume

$$\mathcal{Q}[T] = -\frac{\lambda_{\alpha}}{\pi} \int_0^{\infty} \frac{T(s+z) - T(s-z)}{z^{\alpha}} dz. \quad (1)$$

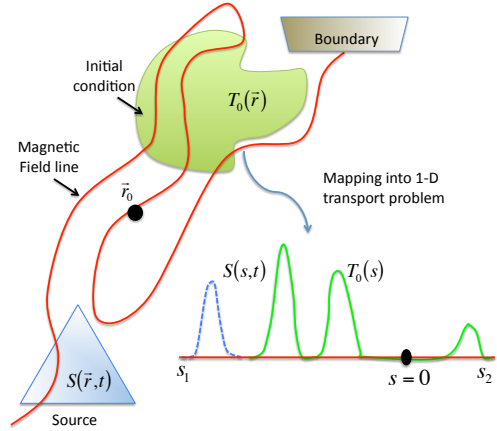


Figure 1: Schematics of Lagrangian-Green's function (LG) method [1,2].

In general $1 \leq \alpha < 2$, but here we limit attention to $\alpha = 1$. Assuming tokamak ordering (i.e., the presence of a dominant toroidal magnetic field component) we approximate $|(\partial_s B)/B| \ll |(\partial_s \mathcal{Q})/\mathcal{Q}|$, and write the parallel transport equation as

$$\partial_t T = -\chi_{\parallel} \partial_s \mathcal{Q} + S. \quad (2)$$

Given a time-independent magnetic field, $\mathbf{B}(\mathbf{r})$, the unique field line path, $\mathbf{r} = \mathbf{r}(s)$, parametrized by the arc-length s , and passing through \mathbf{r}_0 is given by the solution of the initial value problem $\frac{d\mathbf{r}}{ds} = \hat{\mathbf{b}}, \mathbf{r}(s=0) = \mathbf{r}_0$. As illustrated in Fig. 1, the LG method [1,2] is based on the fact that, when $\mathbf{q}_{\perp} = 0$, given an initial temperature distribution $T_0(\mathbf{r}) = T(\mathbf{r}, t=0)$, and a source $S(\mathbf{r}, t)$, the temperature at a given point in space \mathbf{r}_0 , at a time t , is obtained by summing all the contributions of the initial condition and the source along the magnetic field line path:

$$T(\mathbf{r}_0, t) = \int_{-\infty}^{\infty} T_0 [\mathbf{r}(s')] \mathcal{G}(s', t) ds' + \int_0^t dt' \int_{-\infty}^{\infty} ds' S [\mathbf{r}(s'), t'] \mathcal{G}(s', t-t'), \quad (3)$$

where \mathcal{G} is the Green's function of the parallel transport equation. A key feature of the LG method is that the computation of T at \mathbf{r}_0 at time t does not require the computation of T in the neighborhood of \mathbf{r}_0 , as it is the case in finite difference methods, or the computation of T at previous times.

III. Shearless Cantori partial barriers in reversed shear configuration. From the dynamical systems perspective, magnetic fields with non-monotonic q -profiles correspond to nontwist Hamiltonian systems known to exhibit very robust transport barriers [4]. As a result, reversed magnetic field configurations typically have barriers to chaotic magnetic field line transport in the vicinity of the extrema of the q -profile (i.e. shearless regions of the magnetic field). Our goal is to study the role of these shearless barriers in the transport of temperature. The magnetic field used in this study consists of a helical magnetic field with a non-monotonic q -profile with a single minimum superimposed with twenty one strongly overlapping modes. Figure 2(a)

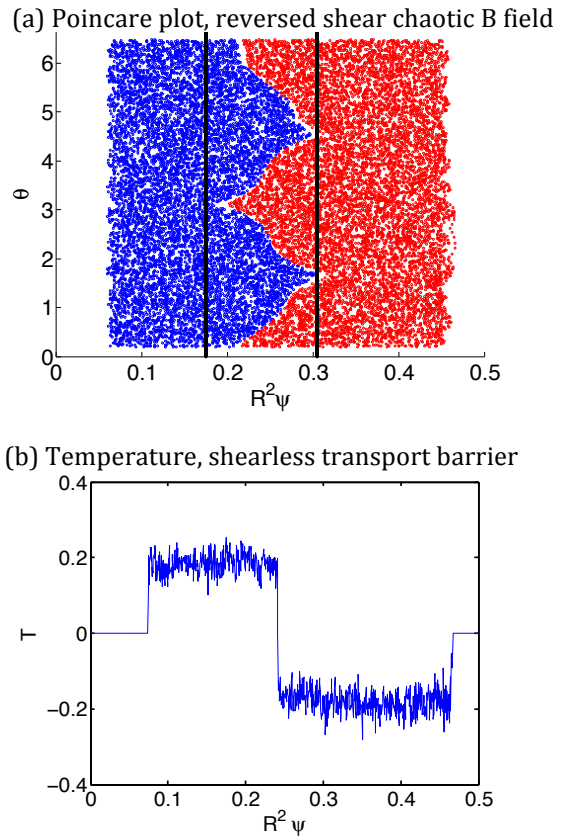


Figure 2: Temperature transport barrier in reversed shear configuration.

shows a Poincare plot for the case when the amplitude of the modes is just below the critical amplitude for the onset of global chaos. The magnetic field exhibits two strongly chaotic transport regions (depicted with red and blue dots) separated by a robust shearless transport barrier. As expected, the resulting radial temperature profile (obtained from the numerical solution of the anisotropic transport equation using the LG method) exhibits two plateaus of well mixed temperature separated by a strong gradient. Figure 3 shows the evolution of an initial linear radial profile for the case when the amplitudes of the modes are just above the critical threshold for the destruction of the shearless transport barrier. Although in this case there are no transport barriers in the system, the relaxation of the temperature is extremely small due to the presence of shearless Cantori. As shown in the left panel of Fig.3, in the early stages, the shearless Cantori reduce the flux and give rise to a partial transport barrier in the reversed shear region, $q' = 0$. At later times, in direct contradiction with the Fourier-Fick's prescription, the flux remains finite in regions where the temperature gradient is zero.

IV. Nondiffusive self-similar scaling and non-local effective radial transport

To explore in more detail the role of shearless Cantori, we consider the transport of localized temperature pulse perturbation of the form $T_0(\psi) = \exp[-(R^2\psi - 0.25)^2/\sigma_0^2]$, with $\sigma_0 = 0.02$. Figure 4 shows the resulting radial temperature profiles for different parallel closures and different magnetic field line configurations obtained from the solution of the parallel heat transport equation. In Refs. [1,2] it was observed that in the case of monotonic q -profiles the temperature exhibits self-similar spatio-temporal evolution of the form $\langle T \rangle(\psi, t) = (\chi_{\parallel} t)^{-\gamma/2} L_{\alpha}(\eta)$ where $\eta = (\psi - \bar{\psi})/(\chi_{\parallel} t)^{\gamma/2}$ is the similarity variable and γ the scaling exponent. As shown in Fig.4(a), for monotonic q -profiles with local (diffusive) parallel closure, the scaling function is an stretched exponential $L_2(\eta) = A e^{-|\eta/\mu|^v}$ with $v \approx 1.6$. But for monotonic q -profiles with non-local closure, the scaling function exhibits heavy tails well fitted by $L_1(\eta) = \frac{A}{2} \left[\frac{1+e^{-\eta^2/\sigma^2}}{1+|\eta/\mu|^3} \right]$. As Figs.4(c) and 4(d) show, these fittings hold in the vicinity of $q' = 0$ in the reversed shear configuration, with the interesting exception that in the local closure case the scaling function becomes exponential (i.e., in this case $v = 1$).

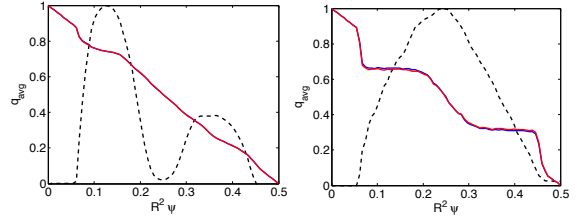


Figure 3: Temperature transport in the presence of shearless Cantori transport barrier. Left panel shows the temperature (solid line) and the flux (dashed line) at $t = 100$. Right panel shows the same for $t = 5 \times 10^5$.

In the standard diffusion paradigm, the Fourier-Fick's prescription implies that the radial heat flux, $\langle \mathbf{q} \cdot \hat{e}_\psi \rangle$, and the radial temperature gradient, $\langle \nabla T \cdot \hat{e}_\psi \rangle$, averaged over z and θ , satisfy $\langle \mathbf{q} \cdot \hat{e}_\psi \rangle = -\chi_{eff} \langle \nabla T \cdot \hat{e}_\psi \rangle$, where χ_{eff} is the effective diffusivity, and $\hat{e}_\psi = \hat{e}_r$ is the unit vector in the radial direction. To test the applicability of this relation for temperature transport in reversed shear chaotic magnetic fields we computed the radial flux and the radial temperature gradient as functions of the radial flux variable, ψ , at fixed time. In direct contradiction with the Fourier-Fick's prescription, Fig. 5 exhibits regions where the temperature gradient is zero but the flux is finite. Figure 5 also shows that the parametric curves $\mathcal{C} : \psi \rightarrow [-\langle \nabla T \cdot \hat{e}_\psi \rangle(\psi), \langle \mathbf{q} \cdot \hat{e}_\psi \rangle(\psi)]$ in the flux-gradient plane, exhibit multivalued loops which provides further evidence of the inapplicability of the Fourier-Fick's prescription with constant effective radial diffusivity, χ_{eff} .

Acknowledgments. This work

was sponsored by the Oak Ridge National Laboratory, managed by UT-Battelle, LLC, for the U.S. Department of Energy under contract DE-AC05-00OR22725.

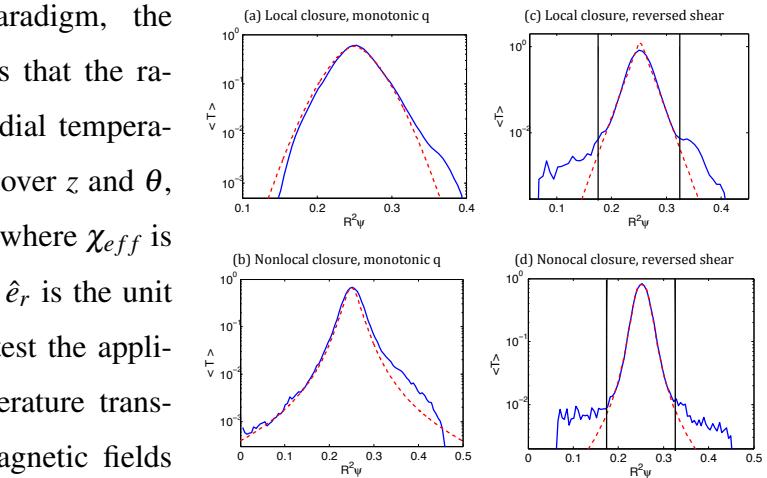
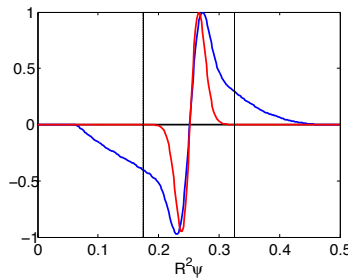


Figure 4: Comparison between numerically computed temperature profiles (solid blue) and self-similar models (dashed red).



References

- [1] D. del-Castillo-Negrete, and L. Chacón, Phys. Rev. Lett., **106**, 195004 (2011).
- [2] D. del-Castillo-Negrete, and L. Chacón, Phys. Plasmas **19**, 056112 (2012).
- [3] D. Blazevski, and D. del-Castillo-Negrete, "Transport barriers and shearless Cantori in reversed shear magnetic field line configurations" Preprint (2012).
- [4] D. del-Castillo-Negrete, J. M. Greene, and P. J. Morrison, Physica D **91**, 1-23 (1996).